Structural Engineering and Mechanics, *Vol. 51, No. 2 (2014) 333-347*
DOI: http://dx.doi.org/10.12989/sem.2014.51.2.333

Large deflection analysis of point supported super-elliptical plates

Murat Altekin*

Department of Civil Engineering, Yildiz Technical University, Esenler 34220, Istanbul, Turkey

(Received August 23, 2013, Revised April 3, 2014, Accepted May 18, 2014)

Abstract. Nonlinear bending of super-elliptical plates of uniform thickness under uniform transverse pressure was investigated by the Ritz method. The material was assumed to be homogeneous and isotropic. The contribution of the boundary conditions at the point supports was introduced by the Lagrange multipliers. The solution was obtained by the Newton-Raphson method. The influence of the location of the point supports on the central deflection was highlighted by sensitivity analysis. An approximate relationship between the central deflection and the super-elliptical power was obtained using the method of least squares. The critical points where the maximum deflection may develop, and the influence of nonlinearity were highlighted. The nonlinearity was found to be sensitive to the aspect ratio. The accuracy of the algorithm was validated by comparing the central deflection with the solutions of elliptical and rectangular plates.

Keywords: super-elliptical; plate; nonlinear; bending; large deflection

1. Introduction

If the deflection of a plate is beyond a certain level (i.e., $w \geq 0.3t$) the relation between external load and deflection is no longer linear (Szilard 2004). It is well known that when the deflections are of the same order as the thickness, the membrane forces play a more significant role in carrying the load (Alwar and Nath 1976, Gorji and Akileh 1990), and thus, the analysis must be extended to include the additional effects produced by large deflections (Szilard 2004).

The nonlinear analysis of plates has been a challenging topic in applied mechanics due to the coupled governing differential equations. Since closed form solutions are only available for a limited number of cases depending on the geometry, boundary conditions, material properties, and loading, the problem involving nonlinearity has been attacked by means of various numerical methods (Silverman and Mays 1972, Civalek 2005, Malekzadeh 2007, Dai *et al*. 2013).

Plates of various shapes have been studied by different methods using several plate theories (Mukhopadhyay and Bera 1994, Bayer *et al*. 2002, Özkul and Türe 2004, Artan and Lehmann 2009, Orakdöğen *et al* 2010, Kutlu and Omurtag 2012, Chen 2013). As far as the author knows, in the literature devoted to the nonlinear analysis of plates, except the only paper in which clamped and simply supported boundaries were examined (Zhang 2013), no study has been published on the large deflection of super-elliptical plates. Super-elliptical plates include a large variety of plate

*Corresponding author, Associate Professor, E-mail: altekin@yildiz.edu.tr

http://www.techno-press.org/?journal=sem&subpage=8 ISSN: 1225-4568 (Print), 1598-6217 (Online)

shapes ranging from an ellipse to a rectangle with rounded corners. Rectangular plates with rounded corners enable to diffuse and dilute stress concentrations unlike plates with sharp corners (Liew *et al*. 1998). However, although they are extensively used as structural and machine elements in aviation, shipbuilding, bridge construction and in applications of aerospace and naval engineering where the deflections are no longer small (Zhang and Kim 2006), the number of studies dealing with them has been rather limited (Asemi *et al*. 2013, Ceribasi 2013, Hasheminehad *et al*. 2013, Jazi and Farhatnia 2012, Tang *et al*. 2012, Algazin 2011, Wu and Liu 2005, Zhou *et al*. 2004, Pedersen 2004, Liew and Feng 2001, Chen *et al*. 1999, Lim *et al*. 1998, Wang *et al*. 1994, and the references cited therein). Besides, plates resting on isolated points such as telescope mirrors, solar panels, printed circuit boards, or slabs supported by columns are frequently encountered in structural design. In the current study the nonlinear bending behavior of a super-elliptical plate undergoing large deflection, and supported symmetrically by four intermediate point supports on the diagonals was examined. Sensitivity analysis was made to determine the influence of the position of the point supports on the maximum deflection. Since the bending moments are crucial in design, the support location minimizing the bending moments at the supports and at the center of the plate was investigated. The large deflection bending response of the plate was compared with the linear solution, and the influence of the thickness on the central deflection was observed. Some of the numerical results were presented for future reference. The accuracy of the algorithm was checked with the solutions of elliptical and rectangular plates, and good agreement was obtained.

2. Formulation

In Cartesian coordinates the boundary contour of a super-elliptical plate can be defined by (Liew *et al*. 1998)

$$\left(\frac{x}{a}\right)^{2k}+\left(\frac{y}{b}\right)^{2k}=1, \qquad k=1,2,\ldots,\infty \tag{1}$$

The strain energy of the plate due to bending, the strain energy of the plate due to strain of the middle surface, the potential energy of the lateral load, and the bending moments can be written as (Timoshenko and Woinowsky-Krieger 1959)

$$V_1=\frac{D}{2}\int_{x_1}^{x_2}\int_{y_1}^{y_2}\left\{\left[\left(\frac{\partial^2 w}{\partial x^2}\right)+\left(\frac{\partial^2 w}{\partial y^2}\right)\right]^2-2(1-\mu)\left[\left(\frac{\partial^2 w}{\partial x^2}\right)\left(\frac{\partial^2 w}{\partial y^2}\right)-\left(\frac{\partial^2 w}{\partial x\partial y}\right)^2\right]\right\}dx\,dy \tag{2}$$

$$V_2=\frac{Et}{2(1-\mu^2)}\int_{x_1}^{x_2}\int_{y_1}^{y_2}\left\{\begin{aligned}&\left[\left(\frac{\partial u}{\partial x}\right)^2+\left(\frac{\partial u}{\partial x}\right)\left(\frac{\partial w}{\partial x}\right)^2+\left(\frac{\partial v}{\partial y}\right)^2+\left(\frac{\partial v}{\partial y}\right)\left(\frac{\partial w}{\partial y}\right)^2\right]\\&+\frac{1}{4}\left[\left(\frac{\partial w}{\partial x}\right)^2+\left(\frac{\partial w}{\partial y}\right)^2\right]^2\\&+2\mu\left[\left(\frac{\partial u}{\partial x}\right)\left(\frac{\partial v}{\partial y}\right)+\frac{1}{2}\left(\frac{\partial v}{\partial y}\right)\left(\frac{\partial w}{\partial x}\right)^2+\frac{1}{2}\left(\frac{\partial u}{\partial x}\right)\left(\frac{\partial w}{\partial y}\right)^2\right]\end{aligned}\right.\;dx\,dy$$

$$\left. + \frac{(1-\mu)}{2}\left[\begin{array}{l} \left(\frac{\partial u}{\partial y}\right)^2 + 2\left(\frac{\partial u}{\partial y}\right)\left(\frac{\partial v}{\partial x}\right) + \left(\frac{\partial v}{\partial x}\right)^2 \\ +2\left(\frac{\partial u}{\partial y}\right)\left(\frac{\partial w}{\partial x}\right)\left(\frac{\partial w}{\partial y}\right) + 2\left(\frac{\partial v}{\partial x}\right)\left(\frac{\partial w}{\partial x}\right)\left(\frac{\partial w}{\partial y}\right) \end{array}\right]\right\} \tag{3}$$

$$V_3 = -\int_{x_1}^{x_2}\int_{y_1}^{y_2} q\, w\, dx\, dy, \qquad m_x = -D\left(\frac{\partial^2 w}{\partial x^2} + \mu\frac{\partial^2 w}{\partial y^2}\right), \qquad m_y = -D\left(\frac{\partial^2 w}{\partial y^2} + \mu\frac{\partial^2 w}{\partial x^2}\right) \tag{4}$$

$$x_1 = -x_2 = -a, \qquad y_1 = -y_2 = -\frac{b}{a}\sqrt[2k]{a^{2k} - x^{2k}}, \qquad D = \frac{Et^3}{12\left(1-\mu^2\right)} \tag{5}$$

$$W = \frac{w}{t} = \frac{qa^4\alpha}{Dt}, \qquad U = \frac{u}{t}, \qquad V = \frac{v}{t}, \qquad X = \frac{x}{a}, \qquad Y = \frac{y}{b} \tag{6}$$

$$Q = \frac{q}{E}, \qquad c = \frac{a}{b}, \qquad e = \frac{t}{a}, \qquad X_2 = 1, \qquad Y_2 = \sqrt[2k]{1 - X^{2k}} \tag{7}$$

$$M_x = \frac{a}{D}m_x, \qquad M_y = \frac{a}{D}m_y, \qquad \alpha_x = \frac{D}{a^3 q}M_x, \qquad \alpha_y = \frac{D}{a^3 q}M_y \tag{8}$$

Hence, substituting the non-dimensional variables into Eqs. (2)-(4)

$$V_1 = \frac{Et^3}{2\left(1-\mu^2\right)c}\int_0^{X_2}\int_0^{Y_2}\left\{\begin{array}{l} \frac{e^2}{12}\left(\frac{\partial^2 W}{\partial X^2}\right)^2 + \frac{c^4 e^2}{12}\left(\frac{\partial^2 W}{\partial Y^2}\right)^2 + \frac{c^2 e^2}{6}\left(\frac{\partial^2 W}{\partial X^2}\right)\left(\frac{\partial^2 W}{\partial Y^2}\right) \\ -\frac{(1-\mu)c^2 e^2}{6}\left[\left(\frac{\partial^2 W}{\partial X^2}\right)\left(\frac{\partial^2 W}{\partial Y^2}\right) - \left(\frac{\partial^2 W}{\partial X\,\partial Y}\right)^2\right] \end{array}\right\} dX\, dY \tag{9}$$

$$V_2 = \frac{Et^3}{2\left(1-\mu^2\right)c}\int_0^{X_2}\int_0^{Y_2}\left\{\begin{array}{l} \left[\begin{array}{l} \left(\frac{\partial U}{\partial X}\right)^2 + e\left(\frac{\partial U}{\partial X}\right)\left(\frac{\partial W}{\partial X}\right)^2 + c^2\left(\frac{\partial V}{\partial Y}\right)^2 \\ +c^3 e\left(\frac{\partial V}{\partial Y}\right)\left(\frac{\partial W}{\partial Y}\right)^2 \end{array}\right] \\ +\frac{e^2}{4}\left[\left(\frac{\partial W}{\partial X}\right)^4 + c^4\left(\frac{\partial W}{\partial Y}\right)^4 + 2c^2\left(\frac{\partial W}{\partial X}\right)^2\left(\frac{\partial W}{\partial Y}\right)^2\right] \\ +2\mu\left[\begin{array}{l} c\left(\frac{\partial U}{\partial X}\right)\left(\frac{\partial V}{\partial Y}\right) + \frac{ce}{2}\left(\frac{\partial V}{\partial Y}\right)\left(\frac{\partial W}{\partial X}\right)^2 \\ +\frac{c^2 e}{2}\left(\frac{\partial U}{\partial X}\right)\left(\frac{\partial W}{\partial Y}\right)^2 \end{array}\right] \end{array}\right. dX\, dY$$

$$\left. + \frac{(1-\mu)}{2} \left[\begin{array}{l} c^2 \left(\frac{\partial U}{\partial Y} \right)^2 + 2c \left(\frac{\partial U}{\partial Y} \right) \left(\frac{\partial V}{\partial X} \right) + \left(\frac{\partial V}{\partial X} \right)^2 \\ +2c^2 e \left(\frac{\partial U}{\partial Y} \right) \left(\frac{\partial W}{\partial X} \right) \left(\frac{\partial W}{\partial Y} \right) \\ +2ce \left(\frac{\partial V}{\partial X} \right) \left(\frac{\partial W}{\partial X} \right) \left(\frac{\partial W}{\partial Y} \right) \end{array} \right] \right\} \tag{10}$$

$$V_3 = -\frac{Et^3}{e^2 c} Q \int_0^{X_2} \int_0^{Y_2} W \, dX \, dY \tag{11}$$

$$M_x = -e \left(\frac{\partial^2 W}{\partial X^2} + \mu c^2 \frac{\partial^2 W}{\partial Y^2} \right), \qquad M_y = -e \left(c^2 \frac{\partial^2 W}{\partial Y^2} + \mu \frac{\partial^2 W}{\partial X^2} \right) \tag{12}$$

are obtained. Due to the symmetry of the plate geometry, a quarter of the plate is used in the computations.

3. Ritz method

The plate is considered to be resting on symmetrically distributed four point supports located at the vertices of a concentric rectangle. The positions of the point supports which prevent both deflection and in-plane displacements are defined by

$$d_x = \Delta_1 a, \qquad d_y = \Delta_2 b \tag{13}$$

where d_x and d_y denote the distance from the central axes of the plate (Fig. 1).

The procedure of the Ritz method can be summarized in two steps. First, an admissible solution which satisfies the Dirichlet (essential) boundary conditions and contains unknown coefficients is chosen (Kwon and Bang 2000). The admissable functions must be at least p times differentiable (Monterrubio and Ilanko 2012). Next, the functional into which the assumed solution is substituted is minimized and the unknown coefficients are found (Kwon and Bang 2000). However, if it is difficult to construct a series of assumed functions that satisfies all the prescribed boundary conditions, the Ritz method combined with Lagrange multipliers is employed (Szilard 2004). Therefore, the geometrical boundary conditions at the point support at (X, Y)=(Δ_1, Δ_2) are satisfied by the subsidiary conditions G_1, G_2, G_3 given by (Brebbia 1984)

$$G_1 = W(\Delta_1, \Delta_2), \qquad G_2 = U(\Delta_1, \Delta_2), \qquad G_3 = V(\Delta_1, \Delta_2) \tag{14}$$

Consequently, the modified functional F becomes

$$F = V_1 + V_2 + V_3 + \sum_{i=1}^{3} \lambda_i G_i \tag{15}$$

where λ_1, λ_2, λ_3 are the Lagrange multipliers. The transverse deflection surface W, and the horizontal displacements U, and V are constructed as two dimensional complete polynomials given by

$$W = W(X,Y) = \sum_{m=0}^{d/2}\sum_{n=0}^{m} A_{mn} X^{2n} Y^{2(m-n)}, \qquad U = U(X,Y) = X\sum_{m=0}^{d/2}\sum_{n=0}^{m} B_{mn} X^{2n} Y^{2(m-n)} \tag{16}$$

$$V = V(X,Y) = Y\sum_{m=0}^{d/2}\sum_{n=0}^{m} C_{mn} X^{2n} Y^{2(m-n)}, \qquad r = \frac{(d+2)(d+4)}{8} \tag{17}$$

where the unknowns A_{mn}, B_{mn}, C_{mn} and λ_i are determined from the minimum potential energy principle by (Wang *et al*. 2002)

$$\frac{\partial F}{\partial A_{mn}} = 0, \qquad \frac{\partial F}{\partial B_{mn}} = 0, \qquad \frac{\partial F}{\partial C_{mn}} = 0, \qquad \frac{\partial F}{\partial \lambda_i} = 0, \qquad i = 1,2,3, \tag{18}$$

Eq. (18) yields a system of nonlinear equations due to V_2. The components of linear and nonlinear coefficient matrices C_L, and C_N are introduced by

$$[C_L] = \begin{bmatrix} \left[\dfrac{\partial^2 F_L}{\partial A_{mn}^2}\right]_{rxr} & \left[\dfrac{\partial^2 F_L}{\partial A_{mn}\partial B_{mn}}\right]_{rxr} & \left[\dfrac{\partial^2 F_L}{\partial A_{mn}\partial C_{mn}}\right]_{rxr} & \left[\dfrac{\partial^2 F_L}{\partial A_{mn}\partial \lambda_i}\right]_{rx3} \\ \left[\dfrac{\partial^2 F_L}{\partial B_{mn}\partial A_{mn}}\right]_{rxr} & \left[\dfrac{\partial^2 F_L}{\partial B_{mn}^2}\right]_{rxr} & \left[\dfrac{\partial^2 F_L}{\partial B_{mn}\partial C_{mn}}\right]_{rxr} & \left[\dfrac{\partial^2 F_L}{\partial B_{mn}\partial \lambda_i}\right]_{rx3} \\ \left[\dfrac{\partial^2 F_L}{\partial C_{mn}\partial A_{mn}}\right]_{rxr} & \left[\dfrac{\partial^2 F_L}{\partial C_{mn}\partial B_{mn}}\right]_{rxr} & \left[\dfrac{\partial^2 F_L}{\partial C_{mn}^2}\right]_{rxr} & \left[\dfrac{\partial^2 F_L}{\partial C_{mn}\partial \lambda_i}\right]_{rx3} \\ \left[\dfrac{\partial^2 F_L}{\partial \lambda_i\partial A_{mn}}\right]_{3xr} & \left[\dfrac{\partial^2 F_L}{\partial \lambda_i\partial B_{mn}}\right]_{3xr} & \left[\dfrac{\partial^2 F_L}{\partial \lambda_i\partial C_{mn}}\right]_{3xr} & \left[\dfrac{\partial^2 F_L}{\partial \lambda_i^2}\right]_{3x3} \end{bmatrix} \tag{19}$$

$$[C_N] = \begin{bmatrix} \left[\dfrac{\partial^2 F_N}{\partial A_{mn}^2}\right]_{rxr} & \left[\dfrac{\partial^2 F_N}{\partial A_{mn}\partial B_{mn}}\right]_{rxr} & \left[\dfrac{\partial^2 F_N}{\partial A_{mn}\partial C_{mn}}\right]_{rxr} & \left[\dfrac{\partial^2 F_N}{\partial A_{mn}\partial \lambda_i}\right]_{rx3} \\ \left[\dfrac{\partial^2 F_N}{\partial B_{mn}\partial A_{mn}}\right]_{rxr} & \left[\dfrac{\partial^2 F_N}{\partial B_{mn}^2}\right]_{rxr} & \left[\dfrac{\partial^2 F_N}{\partial B_{mn}\partial C_{mn}}\right]_{rxr} & \left[\dfrac{\partial^2 F_N}{\partial B_{mn}\partial \lambda_i}\right]_{rx3} \\ \left[\dfrac{\partial^2 F_N}{\partial C_{mn}\partial A_{mn}}\right]_{rxr} & \left[\dfrac{\partial^2 F_N}{\partial C_{mn}\partial B_{mn}}\right]_{rxr} & \left[\dfrac{\partial^2 F_N}{\partial C_{mn}^2}\right]_{rxr} & \left[\dfrac{\partial^2 F_N}{\partial C_{mn}\partial \lambda_i}\right]_{rx3} \\ \left[\dfrac{\partial^2 F_N}{\partial \lambda_i\partial A_{mn}}\right]_{3xr} & \left[\dfrac{\partial^2 F_N}{\partial \lambda_i\partial B_{mn}}\right]_{3xr} & \left[\dfrac{\partial^2 F_N}{\partial \lambda_i\partial C_{mn}}\right]_{3xr} & \left[\dfrac{\partial^2 F_N}{\partial \lambda_i^2}\right]_{3x3} \end{bmatrix} \tag{20}$$

where

$$F_L=\sum_{i=1}^{3}\lambda_i\,G_i+\frac{Et^3}{2\left(1-\mu^2\right)c}\int_0^{X_2}\int_0^{Y_2}\left\{\begin{array}{l}\dfrac{e^2}{12}\left(\dfrac{\partial^2W}{\partial X^2}\right)^2+\dfrac{c^4e^2}{12}\left(\dfrac{\partial^2W}{\partial Y^2}\right)^2+\dfrac{c^2e^2}{6}\left(\dfrac{\partial^2W}{\partial X^2}\right)\left(\dfrac{\partial^2W}{\partial Y^2}\right)\\ -\dfrac{(1-\mu)c^2e^2}{6}\left[\left(\dfrac{\partial^2W}{\partial X^2}\right)\left(\dfrac{\partial^2W}{\partial Y^2}\right)-\left(\dfrac{\partial^2W}{\partial X\,\partial Y}\right)^2\right]\\ +\left(\dfrac{\partial U}{\partial X}\right)^2+c^2\left(\dfrac{\partial V}{\partial Y}\right)^2+2\mu c\left(\dfrac{\partial U}{\partial X}\right)\left(\dfrac{\partial V}{\partial Y}\right)\\ +\dfrac{(1-\mu)}{2}\left[c^2\left(\dfrac{\partial U}{\partial Y}\right)^2+2c\left(\dfrac{\partial U}{\partial Y}\right)\left(\dfrac{\partial V}{\partial X}\right)+\left(\dfrac{\partial V}{\partial X}\right)^2\right]\end{array}\right\}dX\,dY \quad (21)$$

$$F_N=\frac{Et^3}{2\left(1-\mu^2\right)c}\int_0^{X_2}\int_0^{Y_2}\left\{\begin{array}{l}e\left(\dfrac{\partial U}{\partial X}\right)\left(\dfrac{\partial W}{\partial X}\right)^2+c^3e\left(\dfrac{\partial V}{\partial Y}\right)\left(\dfrac{\partial W}{\partial Y}\right)^2\\ +\dfrac{e^2}{4}\left[\left(\dfrac{\partial W}{\partial X}\right)^4+c^4\left(\dfrac{\partial W}{\partial Y}\right)^4+2c^2\left(\dfrac{\partial W}{\partial X}\right)^2\left(\dfrac{\partial W}{\partial Y}\right)^2\right]\\ +2\mu\left[\dfrac{ce}{2}\left(\dfrac{\partial V}{\partial Y}\right)\left(\dfrac{\partial W}{\partial X}\right)^2+\dfrac{c^2e}{2}\left(\dfrac{\partial U}{\partial X}\right)\left(\dfrac{\partial W}{\partial Y}\right)^2\right]\\ +\dfrac{(1-\mu)}{2}\left[\begin{array}{l}2c^2e\left(\dfrac{\partial U}{\partial Y}\right)\left(\dfrac{\partial W}{\partial X}\right)\left(\dfrac{\partial W}{\partial Y}\right)\\ +2ce\left(\dfrac{\partial V}{\partial X}\right)\left(\dfrac{\partial W}{\partial X}\right)\left(\dfrac{\partial W}{\partial Y}\right)\end{array}\right]\end{array}\right\}dX\,dY \quad (22)$$

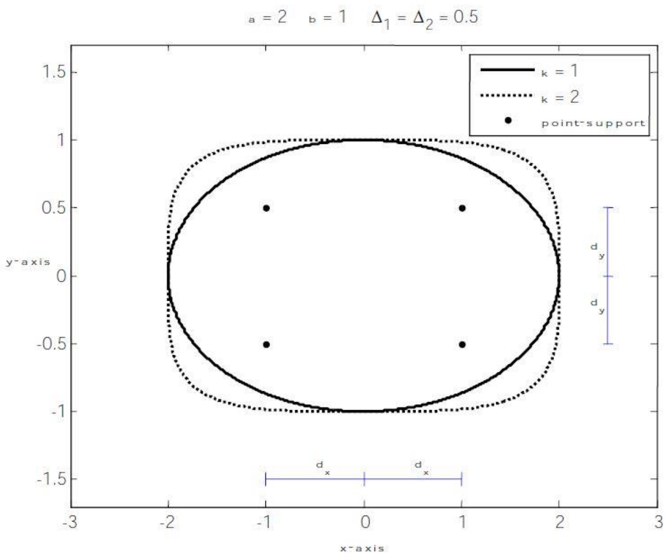

Fig. 1 Geometry of the plate and the location of the point supports

4. Newton-Raphson method

The Newton-Raphson (NR) method is one of the best known iterative techniques in finding the roots of nonlinear equations. The algorithm requires the evaluation of two functions per iteration: the Jacobian matrix which involves the partial derivatives, and the function vector. Depending on the initial guess the NR method may converge fast to the solution. After each iteration, convergence is checked, and the values of the unknowns are updated. The iterations stop when convergence is obtained, and the error is less than the desired tolerance value provided that the maximum number of iterations is not exceeded (Mathews 1992).

In the current paper totally $3r+3$ unknowns were considered, and the zero vector (i.e., the linear solution) was assumed to be the initial guess. For each iteration the Euclidian norm of the function vector was determined, and E_a, and E_r were computed. When $E_a \leq \varepsilon$, or $|E_r| \leq \varepsilon$, the iterations were stopped.

5. Numerical results

The integration with respect to "X" was evaluated numerically by the 12-point Gaussian quadrature technique (Maron and Lopez 1991). The analysis was made for $0.1 \leq \Delta \leq 0.7$ where $\Delta = \Delta_1 = \Delta_2$. Unless otherwise stated the semi-minor axis, the nondimensional load, and the Poisson's ratio were considered to be b=1m, $Q=5\times10^{-10}$, and μ=0.3. As a special case, a corner supported plate was examined for $\Delta = 1/\sqrt[2k]{2}$. Convergence studies were performed and d=8 was found to be sufficient for admissible accuracy. The results of the central deflection computed in the present study for varying support location were compared with those of elliptical (k=1) and rectangular (k=250) plates, and good agreement was obtained (Table 1). The location of the point where the maximum deflection develops was highlighted by comparing the deflections at the points $R_j(X, Y)$ where j=0,1,2,3. The coordinates of these points are $R_0(0,0)$, $R_1(1,0)$, $R_2(0,1)$, $R_3(1/\sqrt[2k]{2}, 1/\sqrt[2k]{2})$. Therefore, the deflections α_0, α_1, α_2, α_3 where the subscripts denote the points R_0, R_1, R_2, R_3, respectively, were computed for varying support location (Table 2). The central deflection of a

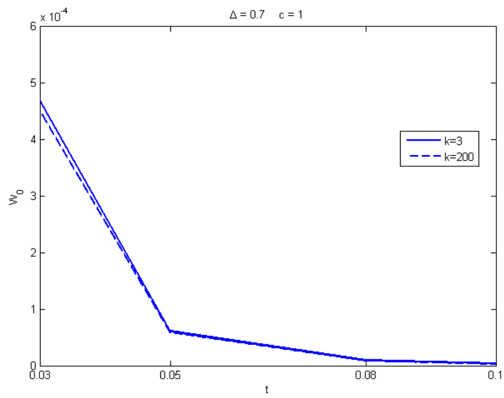

Fig. 2 Influence of the thickness on the cental deflection (c=1)

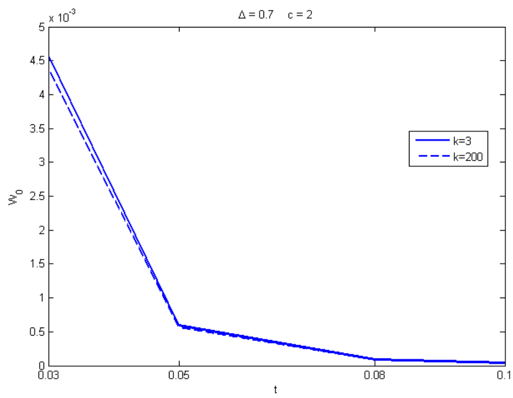

Fig. 3 Influence of the thickness on the cental deflection (c=2)

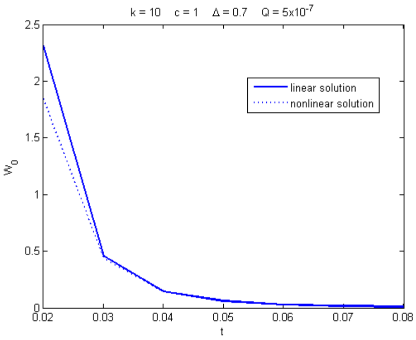

Fig. 4 Comparison of the linear and nonlinear solutions (c=1, Q=5×10^{-7})

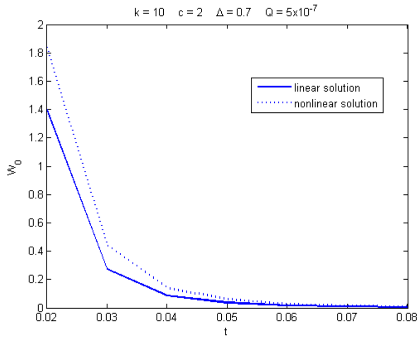

Fig. 5 Comparison of the linear and nonlinear solutions (c=2, Q=5×10^{-7})

Table 1 Convergence study and comparison of the central deflection results for a point-supported super-elliptical plate under uniform pressure (t=0.01 m)

k	c	Δ	μ	d	α_0	Reference	Geometry of the plate
				4	0.0816		
				6	0.0835		
1	1	$1/\sqrt[2k]{2}$	0.17	8	0.0849		Circular plate
					0.0861	(Williams and Brinson 1974)	
					0.0858	(Altekin 2010)	
				4	0.0456		
				6	0.0490		
1	1	$0.9/\sqrt{2}$	0.17	8	0.0491		Circular plate
					0.0500	(Williams and Brinson 1974)	
					0.0499	(Altekin 2010)	
				4	0.4060		
				6	0.4053		
250	1	$1/\sqrt[2k]{2}$	0.28	8	0.4055		Square plate
					0.4052	(Shanmugam *et al*. 1988)	
					0.4060	(Altekin 2010)	
				4	0.4052		
				6	0.4045		
				8	0.4048		
250	1	$1/\sqrt[2k]{2}$	0.30		0.4096	(Wang *et al*. 2002)*	Square plate
					0.4080	(Rajaiah and Rao 1978)	
					0.4052	(Altekin 2010)	
				4	0.0475		
1	2	$1/\sqrt[2k]{2}$	0.30	6	0.0491		Elliptical plate
				8	0.0495		
					0.0497	(Altekin and Altay 2008)	

*The results obtained from Wang *et al*. (2002), Shanmugam *et al*. (1988), and Szilard (1974) were scaled by the author.

Table 1 Continued

20	2	$1/\sqrt[2k]{2}$	0.30	4	0.2123		Super-elliptical plate
				6	0.2132		
				8	0.2134		
					0.2140	(Altekin and Altay 2008)	
250	2	$1/\sqrt[2k]{2}$	1/6	4	0.2227		Rectangular plate
				6	0.2238		
				8	0.2239		
					0.2240	(Szilard 1974)	

Table 2 Location of α_{max} for varying support location (t=0.05, μ=0.3)

c	Δ	α_0	α_1	α_2	α_3
1	Δ=0.1				$\alpha_{max}=\alpha_3$
	0.2≤Δ≤0.4		$\alpha_{max}=\alpha_1$ for k=1		$\alpha_{max}=\alpha_3$ for k≥2
	Δ=0.5		$\alpha_{max}=\alpha_0$ for k≤2		$\alpha_{max}=\alpha_3$ for k≥3
	0.6 Δ≤0.7	$\alpha_{max}=\alpha_0$			
2	0.1≤Δ≤0.4		$\alpha_{max}=\alpha_1$		
	Δ=0.5		$\alpha_{max}=\alpha_1$ for k≥2	$\alpha_{max}=\alpha_2$ for k=1	
	0.6≤Δ≤0.7			$\alpha_{max}=\alpha_2$	

Table 3 Central deflection α_0 for varying support location (c=1, t= 0.05, μ=0.3)

$2k$	Δ=0.1	Δ=0.2	Δ=0.3	Δ=0.4	Δ=0.5	Δ=0.6	Δ=0.7
2	-0.0035	-0.0096	-0.0111	-0.0054	0.0087	0.0341	0.0780
4	-0.0042	-0.0123	-0.0162	-0.0116	0.0023	0.0282	0.0716
6	-0.0044	-0.0131	-0.0178	-0.0137	0.0001	0.0260	0.0696
8	-0.0044	-0.0134	-0.0184	-0.0146	-0.0009	0.0250	0.0687
10	-0.0045	-0.0135	-0.0188	-0.0151	-0.0015	0.0244	0.0681
12	-0.0045	-0.0136	-0.0190	-0.0154	-0.0018	0.0241	0.0678
14	-0.0045	-0.0136	-0.0191	-0.0156	-0.0020	0.0239	0.0676
16	-0.0045	-0.0137	-0.0192	-0.0158	-0.0021	0.0238	0.0675
18	-0.0045	-0.0137	-0.0193	-0.0159	-0.0022	0.0237	0.0674
20	-0.0045	-0.0137	-0.0193	-0.0159	-0.0023	0.0236	0.0673
22	-0.0045	-0.0137	-0.0193	-0.0160	-0.0024	0.0235	0.0672
24	-0.0045	-0.0137	-0.0194	-0.0160	-0.0024	0.0235	0.0672
26	-0.0045	-0.0137	-0.0194	-0.0161	-0.0024	0.0235	0.0672
28	-0.0045	-0.0137	-0.0194	-0.0161	-0.0025	0.0234	0.0671
30	-0.0045	-0.0137	-0.0194	-0.0161	-0.0025	0.0234	0.0671
32	-0.0045	-0.0137	-0.0194	-0.0161	-0.0025	0.0234	0.0671
34	-0.0045	-0.0137	-0.0194	-0.0161	-0.0025	0.0234	0.0671
36	-0.0045	-0.0137	-0.0195	-0.0162	-0.0025	0.0234	0.0671
38	-0.0045	-0.0137	-0.0195	-0.0162	-0.0025	0.0234	0.0671
40	-0.0045	-0.0137	-0.0195	-0.0162	-0.0026	0.0233	0.0670
100	-0.0045	-0.0137	-0.0195	-0.0163	-0.0026	0.0233	0.0670
400	-0.0045	-0.0137	-0.0195	-0.0163	-0.0027	0.0233	0.0670

Table 4 Central deflection α_0 for varying support location (c=2, t=0.05, μ=0.3)

$2k$	Δ=0.1	Δ=0.2	Δ=0.3	Δ=0.4	Δ=0.5	Δ=0.6	Δ=0.7
2	-0.0015	-0.0045	-0.0057	-0.0030	0.0050	0.0206	0.0471
4	-0.0019	-0.0060	-0.0086	-0.0068	0.0008	0.0167	0.0437
6	-0.0021	-0.0065	-0.0095	-0.0082	-0.0007	0.0152	0.0424
8	-0.0021	-0.0067	-0.0099	-0.0088	-0.0014	0.0145	0.0418
10	-0.0021	-0.0068	-0.0101	-0.0091	-0.0017	0.0141	0.0414
12	-0.0022	-0.0068	-0.0103	-0.0093	-0.0019	0.0139	0.0412
14	-0.0022	-0.0069	-0.0103	-0.0094	-0.0021	0.0137	0.0411
16	-0.0022	-0.0069	-0.0104	-0.0095	-0.0022	0.0136	0.0410
18	-0.0022	-0.0069	-0.0104	-0.0095	-0.0022	0.0135	0.0409
20	-0.0022	-0.0069	-0.0104	-0.0096	-0.0023	0.0135	0.0408
22	-0.0022	-0.0069	-0.0105	-0.0096	-0.0023	0.0134	0.0408
24	-0.0022	-0.0069	-0.0105	-0.0096	-0.0023	0.0134	0.0408
26	-0.0022	-0.0069	-0.0105	-0.0096	-0.0024	0.0134	0.0407
28	-0.0022	-0.0069	-0.0105	-0.0096	-0.0024	0.0134	0.0407
30	-0.0022	-0.0069	-0.0105	-0.0097	-0.0024	0.0134	0.0407
32	-0.0022	-0.0069	-0.0105	-0.0097	-0.0024	0.0133	0.0407
34	-0.0022	-0.0069	-0.0105	-0.0097	-0.0024	0.0133	0.0407
36	-0.0022	-0.0069	-0.0105	-0.0097	-0.0024	0.0133	0.0407
38	-0.0022	-0.0070	-0.0105	-0.0097	-0.0024	0.0133	0.0407
40	-0.0022	-0.0070	-0.0105	-0.0097	-0.0024	0.0133	0.0407
100	-0.0022	-0.0070	-0.0106	-0.0097	-0.0025	0.0133	0.0406
400	-0.0022	-0.0070	-0.0106	-0.0097	-0.0025	0.0132	0.0406

Table 5 Coefficients determined by the method of least squares (c=1, t=0.05)

Δ	h_1	h_2	h_3	h_4
0.1	-0.0041263	-1.8096×10^{-5}	1.8797×10^{-7}	-3.6212×10^{-10}
0.2	-0.012063	-8.5564×10^{-5}	8.7633×10^{-7}	-1.6823×10^{-9}
0.3	-0.015762	-0.00018558	1.8827×10^{-6}	-3.6056×10^{-9}
0.4	-0.011129	-0.00025066	2.5317×10^{-6}	-4.8431×10^{-9}
0.5	0.0027313	-0.00026279	2.6557×10^{-6}	-5.0811×10^{-9}
0.6	0.028503	-0.00025617	2.5902×10^{-6}	-4.9563×10^{-9}
0.7	0.072139	-0.00025284	2.5559×10^{-6}	-4.8903×10^{-9}

Table 6 Coefficients determined by the method of least squares (c=2, t=0.05)

Δ	h_1	h_2	h_3	h_4
0.1	-0.0019079	-1.3608×10^{-5}	1.3914×10^{-7}	-2.6701×10^{-10}
0.2	-0.0058758	-5.4293×10^{-5}	5.5282×10^{-7}	-1.0597×10^{-9}
0.3	-0.0083431	-0.00010988	1.1145×10^{-6}	-2.1342×10^{-9}
0.4	-0.0065945	-0.00015446	1.563×10^{-6}	-2.9913×10^{-9}
0.5	0.0010771	-0.00017536	1.7732×10^{-6}	-3.393×10^{-9}
0.6	0.016854	-0.00017587	1.7759×10^{-6}	-3.3969×10^{-9}
0.7	0.043857	-0.00015756	1.587×10^{-6}	-3.0338×10^{-9}

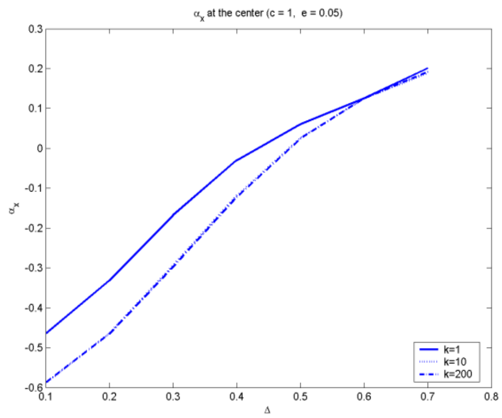

Fig. 6 α_x at the center (c=1, Q=5×10^{-10})

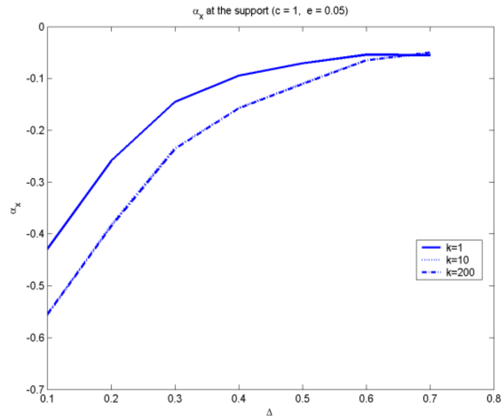

Fig. 7 α_x at the support (c=1, Q=5×10^{-10})

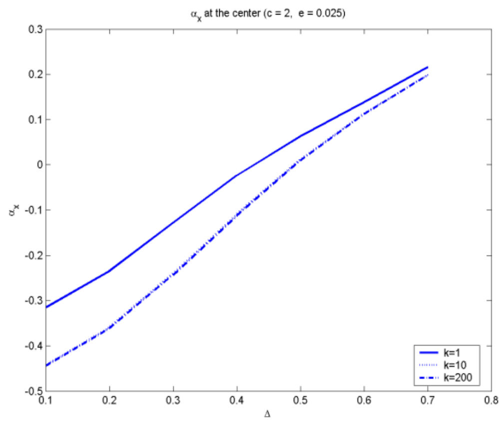

Fig. 8 α_x at the center (c=2, Q=5×10^{-10})

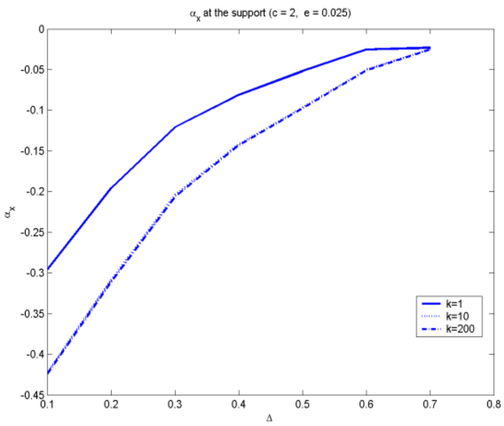

Fig. 9 α_x at the support (c=2, Q=5×10^{-10})

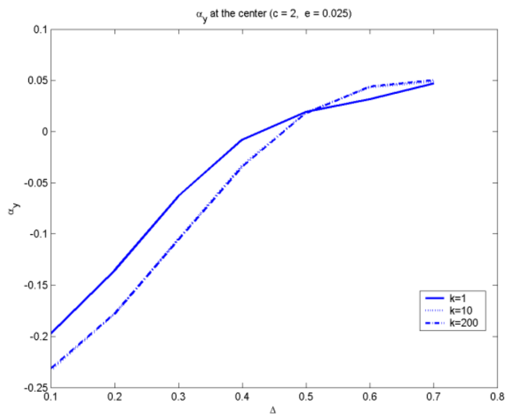

Fig. 10 α_y at the center (c=2, Q=5×10^{-10})

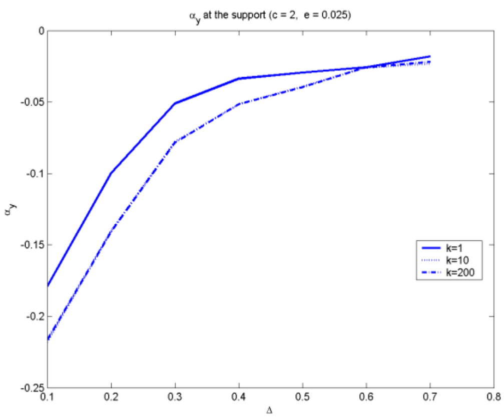

Fig. 11 α_y at the support (c=2, Q=5×10^{-10})

super-elliptical plate undergoing large deflection was presented for future reference (Tables 3-4). The influence of the thickness on the central deflection was investigated for four different values of t as shown on the horizontal axes of Figs. 2-3. The contribution of the nonlinearity on the central deflection was highlighted for 0.02 m$\leq t \leq$0.08 m (Figs. 4-5). The influence of the support location on the bending moment was examined for $0.1\leq\Delta\leq0.7$ (Figs. 6-11).

6. Conclusions

It can be deduced that the perimeter of the plate is more critical than the center in terms of deflection, and the central deflection becomes dominant if $\Delta>0.5$ and $c=1$ (Table 2). The results reveal that $\Delta\cong 0.5$ yields the minimum absolute central deflection for $k>1$ (Tables 3-4). The influence of the super-elliptical power on the central deflection tends to weaken for $k>10$. For practical considerations the central deflection computed for $k=15$ for varying support location may be assumed to be the central deflection of a rectangular plate (Tables 3-4). The central deflection of a super-elliptical plate subject to fully applied uniform transverse pressure can be estimated approximately by the relationship given by

$$\alpha_0 = h_1 + h_2\beta + h_3\beta^2 + h_4\beta^3, \qquad \beta = 2k \tag{23}$$

where h_1, h_2, h_3, h_4 are the scalar coefficients which may be determined by the method of least squares (Tables 5-6).

The relation between the thickness and the central deflection is observed to be nonlinear. The influence of the super-elliptical power on the central deflection decreases if the thickness is raised (Figs. 2-3). The nonlinearity becomes significant for $W_0>0.5$ for $c=1$, and $W_0>0.4$ for $c=2$ (Figs. 4-5). The nonlinearity is observed to be sensitive to the aspect ratio.

As Δ is raised, the influence of k on M_x to be developed at the center and at the support decreases (Figs. 6-11). $\Delta\cong 0.45$, and $\Delta\cong 0.67$ can be considered to be the optimum positions of the point support which minimize the bending moments at the supports and at the center of the plate (Figs. 6-11). The influence of the super-elliptical power on the bending moments α_x, and α_y is negligible for (i) $\Delta\cong 0.6$ (Fig. 6), and $\Delta\cong 0.5$ (Fig. 10) at the center of the plate and (ii) $\Delta\cong 0.66$ (Fig. 7), and $\Delta\cong 0.6$ at the support (Fig. 11). As Δ is raised, the influence of k on the bending moments weakens (Figs. 8-9).

References

Algazin, S.D. (2011), "Vibrations of a free-edge variable-thickness plate of arbitrary shape in plan", *J. Appl. Mech. Tech. Phys.*, **52**(1), 126-131.

Altekin, M. (2010), "Bending of orthotropic super-elliptical plates on intermediate point supports", *Ocean Eng.*, **37**(11-12), 1048-1060.

Altekin, M. and Altay, G. (2008), "Static analysis of point-supported super-elliptical plates", *Arch. Appl Mech.*, **78**(4), 259-266.

Alwar, R.S. and Nath, Y. (1976), "Application of Chebyshev polynomials to the nonlinear analysis of circular plates", *Int. J. Mech. Sci.*, **18**(11-12), 589-595.

Artan, R. and Lehmann, L. (2009), "Initial values method for symmetric bending of micro/nano annular circular plates based on nonlocal plate theory", *J. Comput. Theor. Nanosci.*, **6**(5), 1125-1130.

Asemi, K., Ashrafi, H., Salehi, M. and Shariyat, M. (2013), "Three-dimensional static and dynamic analysis of functionally graded elliptical plates, employing graded finite elements", *Acta Mechanica*, doi: 10.1007/s00707-013-0835-0.

Bayer, I., Guven, U. and Altay, G. (2002), "A parametric study on vibrating clamped elliptical plates with variable thickness", *J. Sound Vib*., **254**(1), 179-188.

Brebbia, C.A. (1984), *The Boundary Element Method for Engineers*, Pentech Press, London, UK.

Ceribasi, S. (2013), "Static and dynamic analysis of thin uniformly loaded super elliptical FGM plates", *Mech. Adv. Mater. Struct*., **19**(5), 325-335.

Chen, C.C., Lim, C.W., Kitipornchai, S. and Liew, K.M. (1999), "Vibration of symmetrically laminated thick super elliptical plates", *J. Sound Vib*., **220**(4), 659-682.

Chen, Y.Z. (2013), "Innovative iteration technique for large deflection problem of annular plate", *Steel Compos. Struct.*, **14**(6), 605-620.

Civalek, Ö. (2005), "Large deflection static and dynamic analysis of thin circular plates resting on two-parameter elastic foundation", *Int. J. Comput. Method*., **2**(2), 271-291.

Dai, H.L., Yan, X. and Yang, L. (2013), "Nonlinear dynamic analysis for fgm circular plates", *J. Mech*., **29**(2), 287-295.

Gorji, M. and Akileh, A.R. (1990), "Elastic-plastic bending of annular plates with large deflection", *Comput. Struct.*, **34**(4), 537-548.

Hasheminejad, S.M., Keshvari, M.M. and Ashory, M.R. (2014), "Dynamic stability of super elliptical plates resting on elastic foundations under periodic ın-plane loads", *J. Eng. Mech*., **140**(1), 172-181.

Jazi, S.R. and Farhatnia, F. (2012), "Buckling analysis of functionally graded super elliptical plate using pb-2 Ritz method", *Adv. Mater. Res*., **383-390**, 5387-5391.

Kutlu, A. and Omurtag, M.H. (2012), "Large deflection bending analysis of elliptic plates on orthotropic elastic foundation with mixed finite element method", *Int. J. Mech. Sci*., **65**(1), 64-74.

Kwon, Y.W. and Bang, H. (2000), *The Finite Element Method using MATLAB*, CRC Press, Boca Raton.

Liew, K.M. and Feng, Z.C. (2001), "Three-dimensional free vibration analysis of perforated super elliptical plates via the p-Ritz method", *Int. J. Mech. Sci*., **43**(11), 2613-2630.

Liew, K.M., Kitipornchai, S. and Lim, C.W. (1998), "Free vibration analysis of thick superelliptical plates", *J. Eng. Mech*., **124**(2), 137-145.

Lim, C.W., Kitipornchai, S. and Liew, K.M. (1998), "A free vibration analysis of doubly connected thick super elliptical laminated composite plates", *Compos. Sci. Tech*., **58**(3-4), 435-445.

Malekzadeh, P. (2007), "A DQ nonlinear bending analysis of skew composite thin plates", *Struct. Eng. Mech.*, **25**(2), 161-180.

Maron, M.J. and Lopez, R J. (1991), *Numerical Analysis: A Practical Approach*, Wadsworth Publishing Company, Belmont.

Mathews, J.H. (1992), *Numerical Methods for Mathematics, Science, and Engineering*, Prentice Hall, Englewood Cliffs, USA.

Monterrubio, L.E. and Ilanko, S. (2012), "Sets of admissable functions for the Rayleigh-Ritz method", *Proceedings of the Eleventh International Conference on Computational Structures Technology*, Dubrovnik, Croatia.

Mukhopadhyay, B. and Bera, R.K. (1994), "Nonlinear analysis of thin homogeneous orthotropic elastic plates under large deflection and thermal loading", *Comput. Math. Appl*., **28**(9), 81-88.

Orakdöğen, E., Küçükarslan, S., Sofiyev, A. and Omurtag, M.H. (2010), "Finite element analysis of functionally graded plates for coupling effect of extension and bending", *Meccanica*, **45**(1), 63-72.

Özkul, T.A. and Türe, Ü. (2004), "The transition from thin plates to moderately thick plates by using finite element analysis and the shear locking problem", *Thin Wall. Struct*., **42**(10), 1405-1430.

Pedersen, N.L. (2004), "Optimization of holes in plates for control of eigenfrequencies", *Struct. Multidisc. Opt.*, **28**(1), 1-10.

Rajaiah, K. and Rao, A.K. (1978), "Collocation solution for point-supported square plates", *J. Appl. Mech*., **45**(2), 424-425.

Shanmugam, N.E., Huang, R., Yu, C.H. and Lee, S.L. (1988), "Uniformly loaded rhombic orthotropic plates

supported at corners", *Comput. Struct.*, **30**(5), 1037-1045.
Silverman, I.K. and Mays, J.R. (1972), "A collocation solution of the nonlinear equations for axisymmetric bending of shallow spherical shells", *J. Franklin Ins.*, **294**(3), 181-192.
Szilard, R. (1974), *Theory and Analysis of Plates*, Prentice Hall, Englewood Cliffs, USA.
Szilard, R. (2004), *Theories and Applications of Plate Analysis*, John Wiley & Sons Inc., Hooboken, USA.
Tang, H.W., Yang, Y.T. and Chen, C.K. (2012), "Application of new double side approach method to the solution of super-elliptical plate problems", *Acta Mechanica*, **223**(4), 745-753.
Timoshenko, S.P. and Woinowsky-Krieger, S. (1959), *Theory of Plates and Shells*, McGraw-Hill International Editions, Singapore.
Wang, C.M., Wang, L. and Liew, K.M. (1994), "Vibration and buckling of super elliptical plates", *J. Sound Vib.*, **171**(3), 301-314.
Wang, C.M., Wang, Y.C. and Reddy, J.N. (2002), "Problems and remedy for the Ritz method in determining stress resultants of corner supported rectangular plates", *Comput. Struct.*, **80**(2), 145-154.
Williams, R. and Brinson, H.F. (1974), "Circular plate on multipoint supports", *J. Franklin Ins.*, **297**(6), 429-447.
Wu, L. and Liu, J. (2005), "Free vibration analysis of arbitrary shaped thick plates by differential cubature method", *Int. J. Mech. Sci.*, **47**(1), 63-81.
Zhang, D. (2013), "Non-linear bending analysis of super-elliptical thin plates", *Int. J. Nonlin. Mech.*, **55**, 180-185.
Zhang, Y.X. and Kim, K.S. (2006), "Geometrically nonlinear analysis of laminated composite plates by two new displacement-based quadrilateral plate elements", *Compos. Struct.*, **72**(3), 301-310.
Zhou, D., Lo, S.H., Cheung, Y.K. and Au, F.T.K. (2004), "3-D vibration analysis of generalized super-elliptical plates using Chebyshev-Ritz method", *Int. J. Solid. Struct.*, **41**(16-17), 4697-4712.

Nomenclature

D, E, F	flexural rigidity, Young's modulus, modified functional
Q, U, V, W	nondimensional uniform pressure, nondimensional horizontal displacement along x-axis, nondimensional horizontal displacement along y-axis, nondimensional deflection
A_{mn}, B_{mn}, C_{mn}	coefficients of the shape functions
C_L, C_N	linear coefficient matrix, nonlinear coefficient matrix
E_a, E_r	absolute error, relative error
G_1, G_2, G_3	subsidiary conditions
M_x, M_y	nondimensional bending moments per unit length of the plate
R_0, R_1, R_2, R_3	the critical points where the maximum deflection may develop
V_1, V_2, V_3	strain energy of the plate due to bending, strain energy of the plate due to strain of the middle surface, potential energy of the lateral load
a, b, c	semi-major axis, semi-minor axis, aspect ratio
d	degree of the complete two-dimensional polynomial function
p	order of the highest differential operator in the functional
e, k, q	parameter of thickness, super-elliptical power, uniform pressure
r, t	number of terms in the shape function, thickness of the undeformed plate
u, v, w	horizontal displacement along x-axis, horizontal displacement along y-axis, deflection
d_x, d_y	half span along x-axis, half span along y-axis
m_x, m_y	bending moments per unit length of the plate

ε, μ	tolerance value, Poisson's ratio
α_j, λ_i	nondimensional deflection (j=0, 1, 2, 3), Lagrange multiplier (i=1, 2, 3)
Δ_1, Δ_2	nondimensional half span parallel to x-axis, nondimensional half span parallel to y-axis